

RESEARCH ARTICLE

Apigetrin alleviates intervertebral disk degeneration by regulating nucleus pulposus cell autophagy

Tao Xu¹ | Hongqi Zhao¹ | Jian Li² | Xuan Fang¹ | Hua Wu¹ | Weihua Hu¹ 

¹Department of Orthopedics, Tongji Hospital, Tongji Medical College, Huazhong University of Science and Technology, Wuhan, Hubei, China

²Department of Orthopaedics, Third Hospital of Shanxi Medical University, Shanxi Bethune Hospital, Shanxi Academy of Medical Sciences, Tongji Shanxi Hospital, Taiyuan, China

Correspondence

Weihua Hu, Department of Orthopedics, Tongji Hospital, Tongji Medical College, Huazhong University of Science and Technology, Wuhan, Hubei, China.
Email: whhu@tjh.tjmu.edu.cn

Funding information

Hubei Provincial Natural Science Foundation of China, Grant/Award Number: 2023AFB646; Knowledge Innovation Program of Wuhan-Basic Research, Grant/Award Number: 2023020201010155

Abstract

Background: Intervertebral disk degeneration (IVDD) is a common spine disease, and inflammation is considered to be one of its main pathogenesis. Apigetrin (API) is a natural bioactive flavonoid isolated from various herbal medicines and shows attractive anti-inflammatory and antioxidative properties; whereas, there is no exploration of the therapeutic potential of API on IVDD. Here, we aim to explore the potential role of API on IVDD in vivo and in vitro.

Methods: In vitro, western blotting, real-time quantitative polymerase chain reaction, and immunofluorescence analysis were implemented to explore the bioactivity of API on interleukin-1 beta (IL-1 β)-induced inflammatory changes in nucleus pulposus cells (NPCs). In vivo, histological staining and immunohistochemistry were employed to investigate the histological changes of intervertebral disk sections on puncture-induced IVDD rat models.

Results: In vitro, API played a crucial role in anti-inflammation and autophagy enhancement in IL-1 β -induced NPCs. API improved inflammation by inhibiting the nuclear factor-kappaB and mitogen-activated protein kinase pathways, whereas it promoted autophagy via the phosphatidylinositol 3-kinase/AKT/mammalian target of the rapamycin pathway. Furthermore, in vivo experiment illustrated that API mitigates the IVDD progression in puncture-induced IVDD model.

Conclusions: API inhibited degenerative phenotypes and promoted autophagy in vivo and in vitro IVDD models. Those suggested that API might be a potential drug or target for IVDD.

KEYWORDS

Apigetrin, autophagy, inflammation, intervertebral disk degeneration, MAPK, NF- κ B, PI3K/AKT/mTOR

1 | INTRODUCTION

Low back pain (LBP) is a prevalent global symptom that affects individuals across all age groups and is recognized as the primary contributor to disability.^{1,2} In the United States alone, the financial burden

Tao Xu and Hongqi Zhao have contributed equally to this work.

This is an open access article under the terms of the [Creative Commons Attribution-NonCommercial-NoDerivs](https://creativecommons.org/licenses/by-nc-nd/4.0/) License, which permits use and distribution in any medium, provided the original work is properly cited, the use is non-commercial and no modifications or adaptations are made.

© 2024 The Authors. *JOR Spine* published by Wiley Periodicals LLC on behalf of Orthopaedic Research Society.

associated with the treatment and rehabilitation of LBP surpassed 134.5 billion US dollars in 2016, positioning it at the top of the list of 154 diseases in terms of economic impact.³ However, most interventions have extremely limited effects. It is widely accepted that intervertebral disk (IVD) degeneration (IVDD) is one of the leading causes of LBP.^{4,5} The IVD is vital to spinal function because it connects the vertebral bodies and provide stability between vertebrae while permitting motion.⁶ The IVD is composed of a gelatinous inner core, the nucleus pulposus, and tough outer rings, the annulus fibrosus.⁷ Disk degeneration occurs consistently with advancing age as a result of disordered metabolism of the extracellular matrix (ECM) and a loss of healthy disk cells.^{6,8,9} More specifically, abnormal catabolism driven by increased expression of inflammatory cytokines, including interleukin-1 beta (IL-1 β), interleukin-6 (IL-6), and tumor necrosis factor alpha (TNF- α), as well as catabolic mediators such as the matrix metalloproteinases (MMPs) family, is the main characteristic of IVDD.¹⁰⁻¹²

Autophagy is believed to be a cytoprotective process through which intracellular proteins and organelles can be renewed and mobilized to fulfill the bioenergetic needs of the cell by generating energy-rich compounds.¹³ It is well known that reduced autophagy can be attributed to degenerative changes and accelerated senescence.^{13,14} Accumulating studies have demonstrated that reduced autophagy triggered by various pathological factors, such as oxidative stress and mechanical stress, leads to aggravation of IVDD.¹⁵⁻¹⁷ Additionally, autophagy is involved in maintaining disk homeostasis and acts by preventing apoptosis and senescence.¹⁸⁻²⁰ Enhancing autophagy in nucleus pulposus cells (NPCs) by multifunctional nanoparticles, circular RNAs, or metformin prominently ameliorates disk degeneration in vitro and in vivo.^{7,21,22} Hence, interventions capable of inducing autophagy seem to be effective in protecting IVDs from degeneration.

Flavonoids are a family of polyphenols derived from natural plants and are widely used to combat cancer, neurodegenerative diseases, inflammation, and aging-related diseases due to their superior antioxidant ability.²³ Apigenin (API) is a natural bioactive flavonoid isolated from various herbal medicines and shows attractive anti-inflammatory and antioxidative properties.²⁴⁻²⁶ Recently, Kim et al. demonstrated that API administration increased various autophagy marker proteins, including microtubule-associated protein 1 light chain 3 beta-II (LC3B-II) and beclin-1, by decreasing the phosphorylation of phosphatidylinositol 3-kinase (PI3K)/AKT/mammalian target of the rapamycin (mTOR) pathway proteins in human gastric adenocarcinoma cancer cells.²⁷ Hence, it can be speculated that API may protect cells from the inflammatory environment and oxidative stress by inducing autophagy.

The aim of this study was to explore the potential effect of API on IL-1 β -induced ECM degradation in NPCs and to determine the role of autophagy in the therapeutic effects of API on IVDD. The findings from in vitro and in vivo results indicate that API exhibits considerable potential as a treatment option for IVDD.

2 | MATERIALS AND METHODS

2.1 | Reagents and materials

API (HY-N0578), 3-Methyladenine (3-MA, HY-19312), JSH-23 (HY-13982), SB203580 (HY-10256A), and dimethyl sulfoxide (HY-Y0320) were obtained from MedChemExpress (Monmouth Junction, USA). Recombinant rat IL-1 β protein was obtained from R&D Systems (Minneapolis, USA). Trypsin (25300054), collagenase II (17101015), and fetal bovine serum (FBS) (16000-044) were purchased from Gibco (New York, USA). Dulbecco's Modified Eagle Medium/Ham's F 12 (DMEM/F12) medium was obtained from HyClone (Utah, USA). Boster (Wuhan, China) provided phosphate buffered saline (PBS, AR0032), Cell Counting Kit-8 (CCK-8, AR1160), radio-immunoprecipitation assay (RIPA, AR0102) lysis buffer, general protease inhibitor cocktail (AR1182-1), phosphatase inhibitor cocktail (AR-1183), tris-buffered saline and tween 20 (TBST, AR0195) solution, CY3 Conjugated AffiniPure Goat Anti-rabbit IgG (H + L) (BA1032), FITC Conjugated AffiniPure Goat Anti-rabbit IgG (H + L) (BA1105), and 4,6-diamino-2-phenyl indole (DAPI, AR1176). Four percentage paraformaldehyde (P1110), toluidine blue (G3660), and safranin O (G1067) were purchased from Servicebio (Beijing, China). 10% (E303-01) and 12% (E304-01) Sodium dodecyl sulfate-polyacrylamide gel electrophoresis (SDS-PAGE) gel and one-step real-time quantitative polymerase chain reaction (RT-qPCR) kit (R333-01) were purchased from Vazyme (Nanjing, China). Polyvinylidene fluoride (PVDF, IPVH00010) was purchased from Millipore (Massachusetts, USA). Bovine serum albumin (BSA, 4240GR100) and Triton X-100 (1139ML100) were purchased from BioFroxx (Einhausen, Germany). Total RNA extraction reagent (9108) was purchased from Takara Bio Inc. (Shiga, Japan). Monomeric red fluorescent protein (mRFP)-green fluorescent protein (GFP)-microtubule-associated protein 1 light chain 3 (LC3) adenovirus (HB-AP210) was obtained from HanBio Technology (Shanghai, China). Primary antibodies against Cyclooxygenase 2 (COX-2, #12282), inducible nitric oxide synthase (iNOS, #13120), autophagy related 5 (Atg5, #12994), Atg 12 (#4180), LC3I/II (#12741), P38 (#8690), Phospho-P38 (#4511), c-Jun N-terminal kinase (JNK, #9252), Phospho-JNK (P-JNK, #4668), extracellular signal-regulated kinase (ERK, #4695), Phospho-ERK (P-ERK, #4377), PI3K (#4229), Phospho-PI3K (P-PI3K, #4228), P65 (#8242), and Phospho-P65 (P-P65, #3033) were bought from Cell Signaling Technology (Beverly, USA) and all were used at a dilution of 1:1000. Proteintech Group (Wuhan, China) supplied primary antibodies against Glyceraldehyde phosphate dehydrogenase (GAPDH, 60004-1-Ig), MMP2 (66366-1-Ig), MMP9 (10375-2-AP), MMP13 (18165-1-AP), Collagen II (28459-1-AP), Aggrecan (13880-1-AP), AKT (60203-2-Ig), Phospho-AKT (P-AKT, 66444-1-Ig), mTOR (66888-1-Ig), Phospho-mTOR (P-mTOR, 67 778-1-Ig), P62 (18420-1-AP), and all were used at a dilution of 1:1000. Antibody against the IL-6 (A14687) was provided by ABclonal (Wuhan, China) and utilized at a dilution ratio of 1:500. Antibody against the MMP-3 (BM4074) was provided by Boster (Wuhan, China) and utilized at a dilution ratio of 1:500.

2.2 | Animals

Sprague–Dawley (SD) rats (6 weeks old, male, 220 ± 20 g) were purchased from Hubei Province Experimental Animal Centre (Wuhan, China). A total of 30 rats were sacrificed for this study, of which 6 were used in vivo experiments and 24 were used in vitro experiments. The study was approved by the Ethics Committee on Animal Experimentation of Tongji Hospital, Tongji Medical College, Huazhong University of Science and Technology.

2.3 | Harvest and culture of primary nucleus pulposus cells

Rat primary NPCs were isolated from the coccygeal vertebrae of 6-week-old male SD rats. In brief, nucleus pulposus tissues were collected under aseptic conditions and then incubated with 0.25% trypsin in a cell incubator for 30 min. Next, the samples were digested with collagenase II in a hybrid furnace for 3 h. Subsequently, the NPCs were cultured in DMEM/F12 medium containing 10% FBS in an incubator with 5% CO₂ at 37°C. NPCs in the first or second passage were prepared for the following study.

2.4 | Safranin O staining and toluidine blue staining

Toluidine blue staining and safranin O staining followed similar protocols. The NPCs were washed with 1× sterile PBS three times and then fixed with 4% paraformaldehyde at room temperature for 15 min. After removing the fixation fluid and washing with PBS, the NPCs were stained with safranin O or toluidine blue solution for 30 min. Then, the reagents were eliminated with PBS. The proteoglycan composition and cellular morphology of NPCs could be observed under a microscope.

2.5 | Cell viability assessment

CCK-8 was used to evaluate the cytoactivity of IL-1β in NPCs treated with or without API or 3-MA. According to a previous study, 5 ng/mL IL-1β was used to create the IVDD cell model.²⁸ Following the protocol, the same number of NPCs were seeded into 96-well plates and treated with IL-1β (5 ng/mL) and/or various concentrations of API (5, 10, 25, 50, and 100 μM) and 3-MA (5 mM) for 24 h. After that, each well was incubated with the CCK-8 reagent for 1 h. Then, a microplate reader (BioTek, USA) was used to measure the absorbance at a wavelength of 450 nm.

2.6 | Western blotting

According to the experimental design, NPCs were treated with IL-1β and API. After three washes with PBS, NPCs were lysed for 30 min on

ice with RIPA lysis buffer (including 1 mM general protease and phosphatase inhibitor cocktail). To purify the protein, the lysate was centrifuged at 12 000 rpm for 30 min at 4°C. A 10% or 12% SDS–PAGE gel was used to separate the proteins, which were transferred to PVDF membranes. The bands were incubated at 4°C for 16 h with the corresponding primary antibodies after blocking in 5% BSA. GAPDH has been demonstrated as an appropriate housekeeping gene for NPCs and was used as an internal reference in all assays.²⁹ After washing with TBST solution for 10 min three times, the protein bands were incubated with secondary antibodies at 37°C for 1 h. Finally, the target bands were detected with an Image Lab System (Bio-Rad, USA). ImageJ software (National Institutes of Health, USA) was used to measure the gray value.

2.7 | Real-time quantitative polymerase chain reaction

According to the protocol, total RNA was purified from NPCs using a total RNA extraction reagent, and the purity and concentration were analyzed with a microplate reader (BioTek, USA). Next, a one-step RT-qPCR kit was used to amplify complementary DNA. Finally, the relative messenger RNA expression was calculated using the 2^{-ΔΔCt} method with GAPDH for normalization.²⁹ The primer sequences can be found in Table 1.

TABLE 1 Primer sequence used in the RT-qPCR experiment.

Gene	Sequence
Rat-Collagen II-F	5'-CGAGGCAGACAGTACCTTG-3'
Rat-Collagen II-R	5'-TGCTCTCGATCTGGTTGTC-3'
Rat-Aggregan-F	5'-CTTCCCAACTATCCAGCCAT-3'
Rat-Aggregan-R	5'-TCACACCGATAGATCCCAGA-3'
Rat-MMP13-F	5'-CAAGCAGCTCCAAAGGCTAC-3'
Rat-MMP13-R	5'-TGGCTTTTGCCAGTGTAGGT-3'
Rat-MMP3-F	5'-GCTCATCCTACCCATTGCAT-3'
Rat-MMP3-R	5'-GCTTCCCTGTCTATCTCAGC-3'
Rat-MMP9-F	5'-TCCTTGAATGTGGATGTTT-3'
Rat-MMP9-R	5'-CGTCCTTGAAGAAATGCAGA-3'
Rat-TNF-a-F	5'-ATGGGCTCCCTCTCATCAGT-3'
Rat-TNF-a-R	5'-GCTTGGTGGTTTGCTACGAC-3'
Rat-IL-6-F	5'-TCTCCGCAAGAGACTCCAG-3'
Rat-IL-6-R	5'-AGCCTCCGACTTGTGAAGT-3'
Rat-COX-2-F	5'-CTCAGCCATGCAGCAAATCC-3'
Rat-COX-2-R	5'-GGGTGGGCTTCAGCAGTAAT-3'
Rat-iNOS-F	5'-CTATCCCAGCCCAACAACAC-3'
Rat-iNOS-R	5'-GTCACATGCAGCTTGTCCAG-3'
Rat-GAPDH-F	5'-GGTGAAGGTCGGTGTGAACG-3'
Rat-GAPDH-R	5'-CTCGCTCCTGGAAGATGGT-3'

Abbreviations: F, Forward; R, Reverse; RT-qPC, Rreal-time quantitative polymerase chain reaction.

2.8 | Immunofluorescence staining

An appropriate number of NPCs were seeded into a 48-well plate to administer different treatments. Then, the cells were fixed with 4% paraformaldehyde for 30 min and infiltrated with 0.2% Triton X-100 for 10 min. After 1 h of blocking in 1% BSA, the cells were incubated with primary antibodies (MMP9, MMP13 and Aggrecan, 1:200) at 4°C for 16 h. Next, the cells were incubated with fluorescent secondary antibodies at room temperature in the dark for 1 h. Afterwards, the cells were treated with DAPI staining fluid for 10 min. Finally, fluorescence images in five high magnification random fields (200×) were obtained utilizing a microscope. The region where the cells are located is selected and the mean fluorescence intensity is measured in the ImageJ software.

2.9 | mRFP-GFP-LC3 adenovirus transfection

mRFP-GFP-LC3 adenoviruses were used to detect autophagic flux. When the cell density was close to 60%, the NPCs were infected with the mRFP-GFP-LC3 adenovirus for 24 h. Following this, the NPCs were treated with IL-1 β and/or API for 24 h. Subsequently, a confocal microscope (Nikon America Inc.) was used to capture the autophagic flux. In the merged images, red spots indicate autophagolysosomes and yellow spots indicate autophagosomes. If the autophagosome and autophagolysosome can fuse normally, then the red fluorescence is more than the yellow fluorescence. If the downstream autophagy is blocked and the autophagosome and autophagolysosome cannot fuse normally, the yellow fluorescence is predominant.

2.10 | IVDD model generation and treatment

According to a previous study, an *in vivo* IVDD model was established by using a 20-gage needle to puncture the tail disk.³⁰ In the present study, 24 h male SD rats (220 \pm 20 g, 6 weeks old) were randomly assigned to two groups: a SHAM group (incising tail skin and suturing) and an IVDD group. Then, rats that received the SHAM procedure were randomly assigned to two groups: the SHAM group and the SHAM + API group. Similarly, rats that underwent the puncture procedure were randomly assigned to two groups: the IVDD group and the IVDD + API group. After surgery, the rats in the SHAM group and the IVDD group were injected with 2 μ L of vehicle, whereas the rats in the SHAM + API group and IVDD + API group were injected with 2 μ L of 50 μ M API. The injection was implemented with a 31-gage microsyringe, the size of which did not result in IVDD as previously reported.³¹ In addition, the injection volume of 2 μ L does not induce degenerative changes of NPCs.³² After 6 weeks, the tails of the rats were collected for histological staining and immunohistochemical (IHC) analysis.

2.11 | Histopathological and immunohistochemical analyses

After fixing with 4% paraformaldehyde for 24 h, each IVD tissue was decalcified with a 10% ethylene diamine tetraacetic acid solution for 4 weeks. The tissue was then dehydrated, embedded, and sectioned to a thickness of 5 mm. Slides of each disk were stained with hematoxylin and eosin (HE) and safranin O/fast green (SOFG). The Orthopedic Research Society spine section initiative grading system was used to evaluate IVD degeneration.³³ In addition, the tissue sections were incubated with primary antibodies (MMP13 and Aggrecan, 1:200) for IHC analysis. All section images were obtained using a microscope. In histomorphological analysis, the image was captured at high magnification fields (40×). In IHC analysis, the number of positive cells was counted in three randomly selected high magnification fields (200×) using ImageJ software.

2.12 | Statistical analysis

The *in vitro* experiment data were repeated at least three times and the *in vivo* experiment data were repeated at least six times. All data are presented as the mean \pm standard deviation (SD) and were analyzed using GraphPad Prism V.8 (GraphPad Software Inc., USA). The normal distribution was assessed using the Shapiro–Wilk test. One-way analysis of variance followed by Tukey post hoc test was used to analyze data between multiple experimental groups that meet the normal distribution. Otherwise, the Kruskal–Wallis test was used. A *p* value <0.05 was considered statistically significant.

3 | RESULTS

3.1 | Identification of rat NPCs *in vitro*

The primary rat NPCs were authenticated through safranin O staining, toluidine blue staining and IHC staining of Collagen II. The cell morphology of primary NPCs was fusiform or polygonal (Figure 1A). The cytoplasm of NPCs was stained blue after toluidine blue staining (Figure 1B). Due to its high content of proteoglycan, the cytoplasm was stained red with safranin O staining (Figure 1C). In addition, immunofluorescence (IF) staining revealed the presence of Collagen II, which emitted red fluorescence in the cytoplasm (Figure 1D).

3.2 | Influences of API on the viability of NPCs and selection of the optimal concentration of API

The structure of the API is shown in Figure 1E. The influence of API on cell viability was examined using a CCK-8 kit. First, NPCs were treated with different concentrations of API (0, 5, 10, 25, 50, and 100 μ M) for 24 h. The results showed that the viability of NPCs was

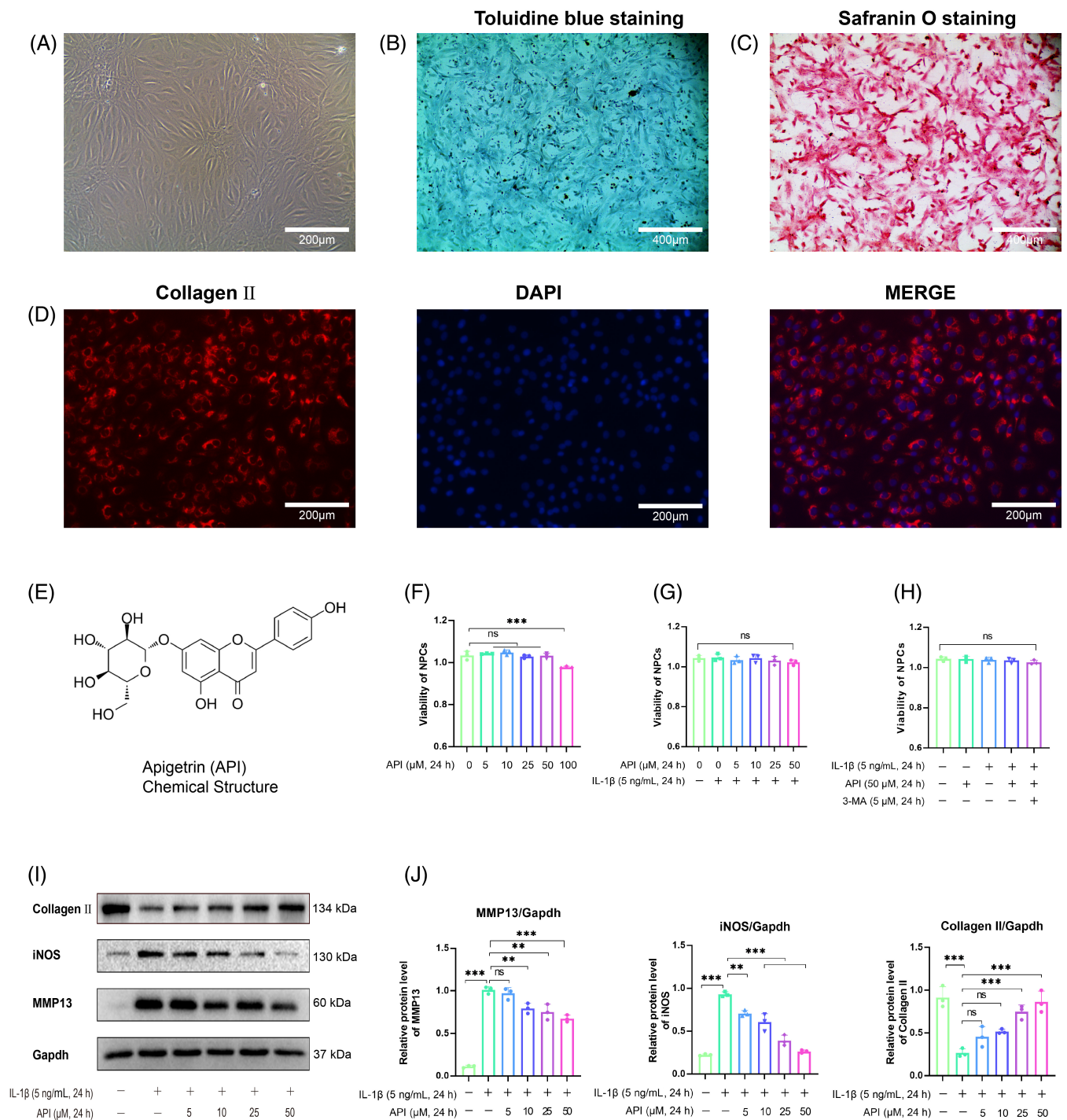


FIGURE 1 Identification of rat nucleus pulposus cells (NPCs) and selection of optimal Apigetrin (API) concentrations. (A) The general shape of primary rat NPCs. (B) Toluidine blue staining and (C) Safranin O staining of primary rat NPCs. (D) Immunofluorescence staining of Collagen II in primary rat NPCs. (E) Chemical structure of API. (F) The CCK8 results showed the viability of NPCs treated with different API concentrations (0, 5, 10, 25, 50, and 100 μM) and (G) with interleukin-1 beta (IL-1 β) (5 ng/mL) alone or with different API concentrations (0, 5, 10, 25, and 50 μM) for 24 h. (H) The viability of NPCs treated with IL-1 β (5 ng/mL), API (50 μM), and 3-MA (5 mM) for 24 h was also measured. (I, J) Western blotting was used to detect the expression of anabolic (Collagen II), catabolic (MMP13), and inflammatory-related (inducible nitric oxide synthase [iNOS]) proteins in NPCs treated with 5 ng/mL IL-1 β alone or in combination with different concentrations of API (5, 10, 25, and 50 μM). Data are shown as the means \pm SD, $n = 3$. * $p < 0.05$; ** $p < 0.01$; *** $p < 0.001$. ns, no significant difference.

significantly inhibited when the concentration of API reached 100 μM (Figure 1F). In addition, there was no significant effect on cell viability after treatment with IL-1 β (5 ng/mL) and API (0, 5, 10, 25, or 50 μM)

for 24 h (Figure 1G). Furthermore, the viability of NPCs was not significantly affected when cells were administered with 5 mM 3-MA for 24 h (Figure 1H). The western blot results showed that 50 μM was

the best concentration of API to enhance anabolism, reduce catabolism, and suppress the inflammatory response (Figure 1I,J). Therefore, 50 μ M API was selected for the follow-up study.

3.3 | API inhibited the inflammatory response in IL-1 β -stimulated NPCs

COX-2, iNOS, and IL-6, the crucial proinflammatory cytokines, are essential for the progression of IVDD.^{34,35} In this study, the protein expression of COX-2, iNOS, and IL-6 was significantly enhanced by IL-1 β stimulation, while this trend was reversed by treatment with 50 μ M API (Figure 2A,B). As shown in Figure 2C, a similar phenomenon was observed at the mRNA level (Figure 2C).

3.4 | API inhibited catabolism in IL-1 β -stimulated NPCs

MMPs, the major matrix-degrading enzymes in the progression of IVDD, are abnormally highly expressed with the stimulation of IL-1 β .^{28,36} Therefore, we detected the protein expression of MMP2, MMP13, MMP9, and MMP3 to analyze the effects of API on catabolism. Western blotting revealed that the increase in MMPs protein levels stimulated by IL-1 β could be decreased by API (Figure 3A,B). As shown in Figure 3C, RT-qPCR demonstrated that the upregulation

of MMP13, MMP9, and MMP3 following stimulation with IL-1 β could be reversed by API. In addition, the IF results clearly showed that the fluorescence intensity of MMP9 and MMP9 in the cytoplasm was significantly higher in the IL-1 β group than in the control group and API alone group. Whereas, API treatment significantly decreased the intensity of MMP9 and MMP13 (Figure 3D,E). These results indicated that API had an anti-catabolic effect in IL-1 β -stimulated NPCs.

3.5 | API promoted anabolism in IL-1 β -stimulated NPCs

Aggrecan and Collagen II are the key elements of the ECM, which are beneficial for disks in resisting compressive loads.³⁷ Therefore, we measured the expression of Aggrecan and Collagen II to analyze the effects of API on anabolism. In this study, the protein expression of Aggrecan and Collagen II was significantly decreased by IL-1 β stimulation, while API alleviated the degeneration of anabolic proteins induced by IL-1 β (Figure 4A,B). RT-PCR also showed that API treatment enhanced the mRNA levels of Aggrecan and Collagen II in IL-1 β -stimulated NPCs (Figure 4C). The IF results further showed that the intensity of Aggrecan in the cytoplasm was significantly lower in IL-1 β -induced NPCs than in the control group and API alone group, whereas API treatment improved the expression of Aggrecan (Figure 4D,E).

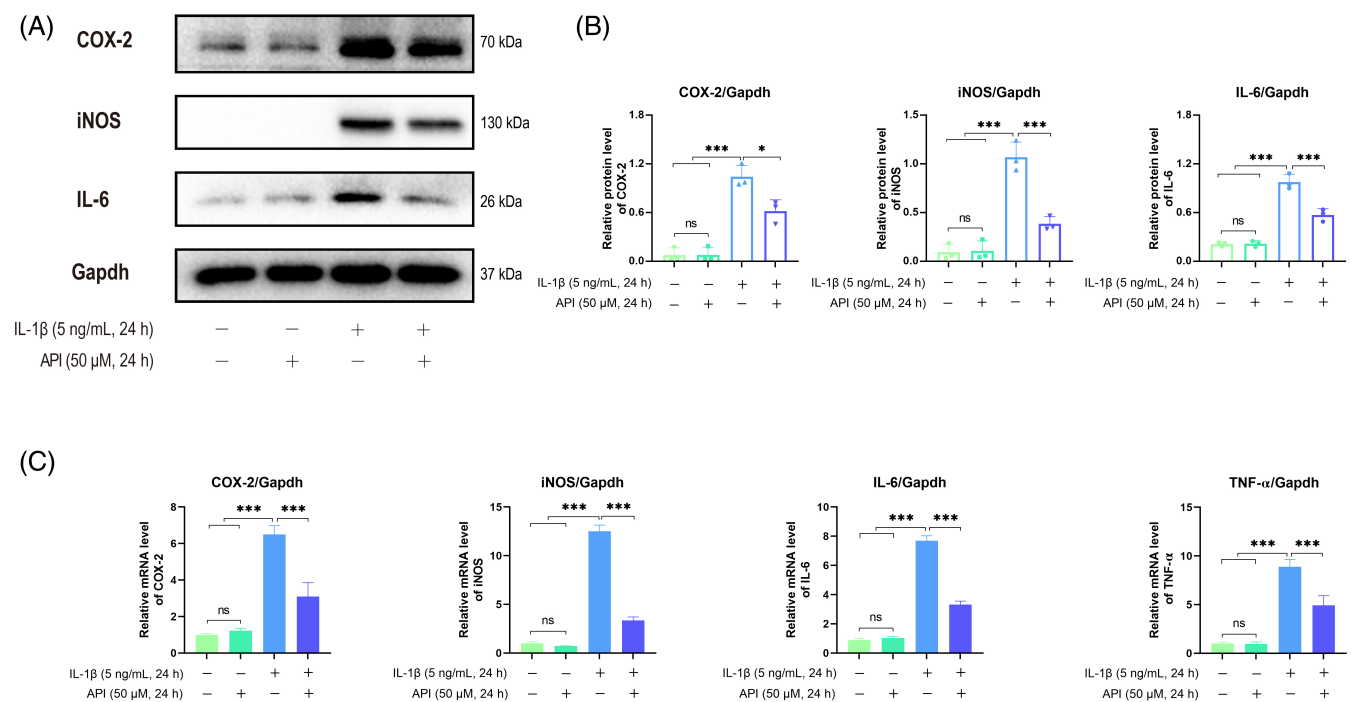


FIGURE 2 Apigenin (API) inhibited the inflammatory responses in interleukin-1 beta (IL-1 β)-stimulated nucleus pulposus cells (NPCs). (A, B) Inflammatory protein expression (inducible nitric oxide synthase [iNOS], Cyclooxygenase 2 [COX-2], and IL-6) in NPCs was shown by western blotting. (C) The mRNA expression levels of inflammatory genes (iNOS, COX-2, IL-6, and TNF- α) were analyzed by real-time quantitative polymerase chain reaction (RT-qPCR). Data are shown as the means \pm SD, $n = 3$. * $p < 0.05$; *** $p < 0.001$. ns, no significant difference.

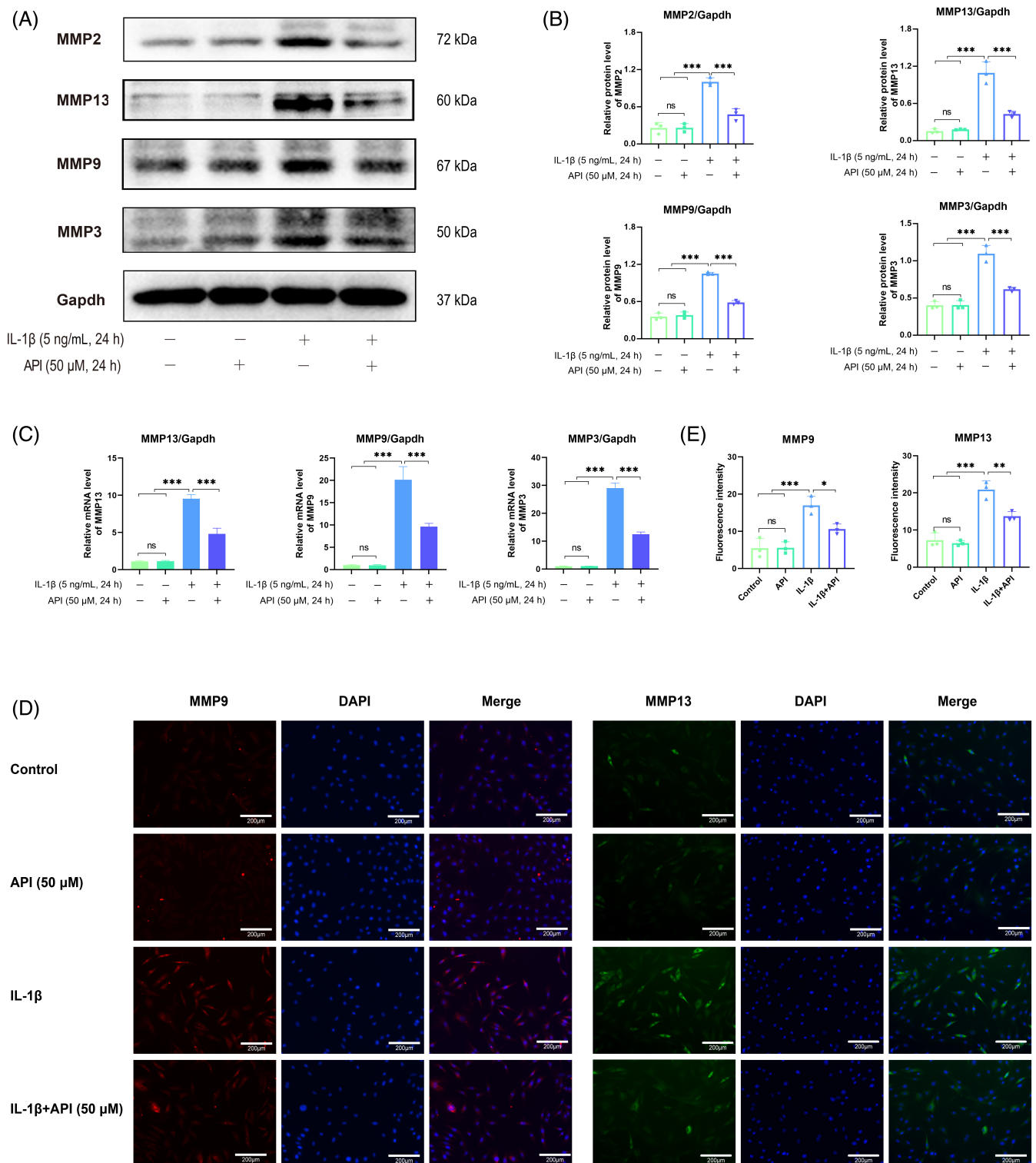


FIGURE 3 Apigetrin (API) inhibits catabolism in interleukin-1 beta (IL-1β)-stimulated nucleus pulposus cells (NPCs). (A, B) The expression of catabolism-related proteins (MMP2, MMP3, MMP9, and MMP13) in NPCs was analyzed by western blotting. (C) The mRNA expression levels of catabolism-related genes (MMP3, MMP9, and MMP13) were analyzed by real-time quantitative polymerase chain reaction (RT-qPCR). (D, E) The expression of MMP9 and MMP13 was detected by immunofluorescence; scale bar = 200 μm. Data are shown as the means ± SD, n = 3.

*p < 0.05; ***p < 0.001; ns, no significant difference. DAPI, 4,6-diamino-2-phenyl indole; IL-1β, interleukin-1 beta; MMP, matrix metalloproteinases.

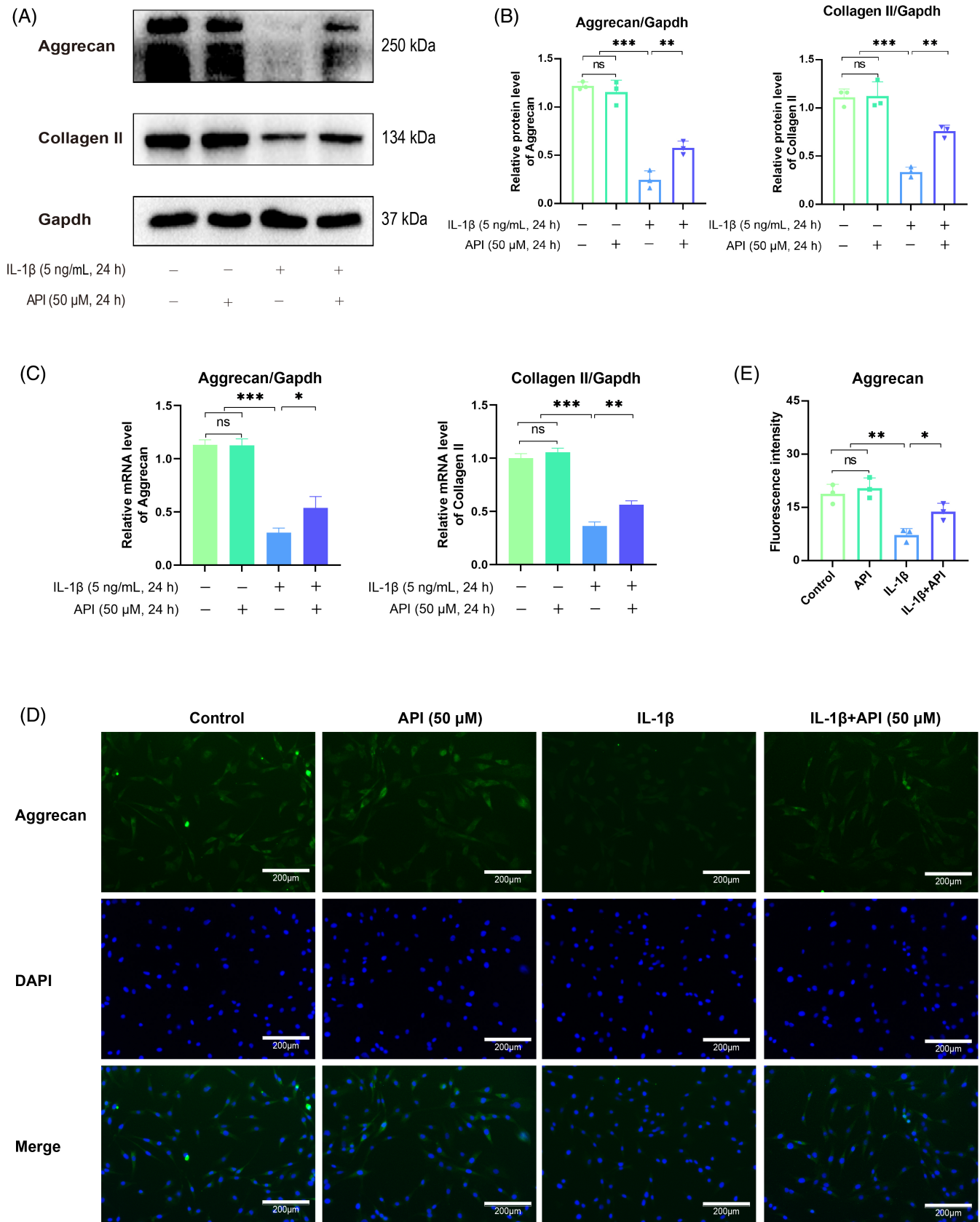


FIGURE 4 Apigetrin (API) promoted anabolism in interleukin-1 beta (IL-1 β)-stimulated nucleus pulposus cells (NPCs). (A, B) The expression of anabolic-related proteins (Aggrecan and Collagen II) in NPCs was analyzed by western blotting. (C) The mRNA expression levels of anabolic-related genes (Aggrecan and Collagen II) were analyzed by real-time quantitative polymerase chain reaction (RT-qPCR). (D, E) Aggrecan expression was detected by immunofluorescence; scale bar = 200 μ m. Data are shown as the means \pm SD, $n = 3$. * $p < 0.05$; ** $p < 0.01$; *** $p < 0.001$. DAPI, 4,6-diamino-2-phenyl indole; IL-1 β , interleukin-1 beta; ns, no significant difference.

3.6 | API inhibited the mitogen-activated protein kinase, nuclear factor-kappaB and PI3K/AKT/mTOR signaling pathways in IL-1 β -stimulated NPCs

Previous studies have found that the mitogen-activated protein kinase (MAPK), nuclear factor-kappaB (NF- κ B), and PI3K/AKT/mTOR signaling pathways play a crucial role in the progression of IVDD.^{20,38–40} Therefore, these three signaling pathways were studied to further explore the mechanisms of API against IVDD. P-P38, P-ERK, P-JNK, and P-P65 were significantly upregulated following IL-1 β stimulation (Figure 5A,B). However, API inhibited the expression of P-P38, P-ERK, P-JNK, and P-P65. Moreover, the expression of P-P65 was accumulated in the nucleus after the stimulation of IL-1 β , while API inhibited this nuclear translocation of P-P65 (Figure 5C,D). We employed pathway inhibitors to block the MAPK and NF- κ B signaling pathways, respectively, and to compare the therapeutic effect of API. In Figure 5E,F, we found that MAPK and NF- κ B pathway inhibitors decreased the expression of iNOS and MMP13 and increased the expression of Collagen II. These results were basically consistent with API treatment, which indirectly suggested that API could partially inhibit inflammation and reverses degenerative phenotypes via inhibiting the MAPK and NF- κ B signaling pathway. Similarly, IL-1 β activated the PI3K/AKT/mTOR signaling pathways, and API treatment suppressed IL-1 β -stimulated phosphorylation of PI3K, AKT, and mTOR (Figure 5F,G).

3.7 | API alleviated impaired autophagy in IL-1 β -stimulated NPCs

Autophagy has been reported to play a key role in the IVDD process.⁴¹ Therefore, we aimed to investigate whether the effect of API on IVDD is related to autophagy. Atg5, Atg12, P62, and LC3II/I are the main autophagy-related proteins. In this study, IL-1 β inhibited the expression of Atg5, Atg12, and LC3II/I while increasing the expression of P62. However, the imbalance in autophagy was mitigated by API treatment (Figure 6A,B). The western blot results were further confirmed with mRFP-GFP-LC3 adenovirus infection (Figure 6C). Then, we used 3-MA, an autophagy inhibitor, to investigate whether blocking the autophagy process attenuates the effect of API on anabolism, catabolism, and the inflammatory response. As shown in Figure 6E,F, we found that 3-MA reversed the enhanced autophagy process induced by API. Furthermore, 3-MA blocked the anti-inflammatory and anti-ECM degradation effects of API.

3.8 | API ameliorated disk degradation in a rat IVDD model

To investigate the effects of API on IVDD in vivo, we punctured the tail disk with a needle to establish a rat model of IVDD. The

results of HE staining and SOFG staining showed that needle puncture caused a remarkable decrease in the number of NPCs, ECM loss, and collapse of the cartilage endplate, whereas API significantly alleviated these pathological changes (Figure 7A–C). Moreover, IHC staining of MMP13 and Collagen II was used to assess the catabolism and anabolism of NPCs. Compared with the SHAM group and SHAM+API group, puncture significantly increased the expression of MMP13 and decreased the expression of Collagen II. However, after API treatment, the percentage of MMP13-positive cells decreased, and the percentage of Collagen II-positive cells increased compared to those in the IVDD group (Figure 7D,E).

4 | DISCUSSION

Currently, some studies have confirmed that degeneration of the IVD is strongly associated with chronic LBP.^{42–44} With advancing age, degenerative disks show an imbalance between anabolic and catabolic processes and gradually lose their function as flexible joints to maintain spine stability. The disturbance of ECM homeostasis is often accompanied by an inflammatory reaction, which in turn exacerbates matrix degeneration in disks. In addition, the occurrence of annulus fibrosus fissures during IVDD leads to nerve ingrowth, which should be inhibited by normal NPCs, and the inflammatory microenvironment further aggravates pain. Finally, spinal instability, inflammation, and neural sensitization resulting from IVDD cause intolerable LBP.⁴⁵ Unfortunately, there is currently no effective treatment available to alleviate disk degeneration and the associated discogenic lumbalgia.⁴⁶

In this study, we identified the protective effects of API on ameliorating IVDD in vitro and in vivo. Consistent with previous studies on different cell types, we found that API showed impressive anti-inflammatory effects on NPCs derived from rats. Meanwhile, similar to other flavonoids, such as quercetin,^{47,48} cardamonin,⁴⁹ and wogonin,⁵⁰ API also significantly inhibited catabolism while promoting anabolism in degenerative IVD. We further confirmed that the beneficial effects could be largely attributed to autophagy induced by API. This is supported by elevated autophagy marker proteins induced by API administration and the attenuated benefits of API on IL-1 β -challenged NPCs after 3-MA administration. In addition, API significantly ameliorated disk degradation in a rat IVDD model. The CCK-8 results showed that there was no significant effect on cell viability after treatment with API (0, 5, 10, 25, or 50 μ M). However, the viability of NPCs was significantly inhibited when the concentration of API reached to 100 μ M. Therefore, we selected the concentration of 50 μ M API for the in vivo experiment. These results provide proof of principle that API may be useful in mitigating disk degeneration by enhancing autophagy to decrease matrix degradation and inflammation in NPCs.

Fuchs et al. first reported that API showed prominent anti-inflammatory activity in combating rat dermatitis.⁵¹ As mentioned

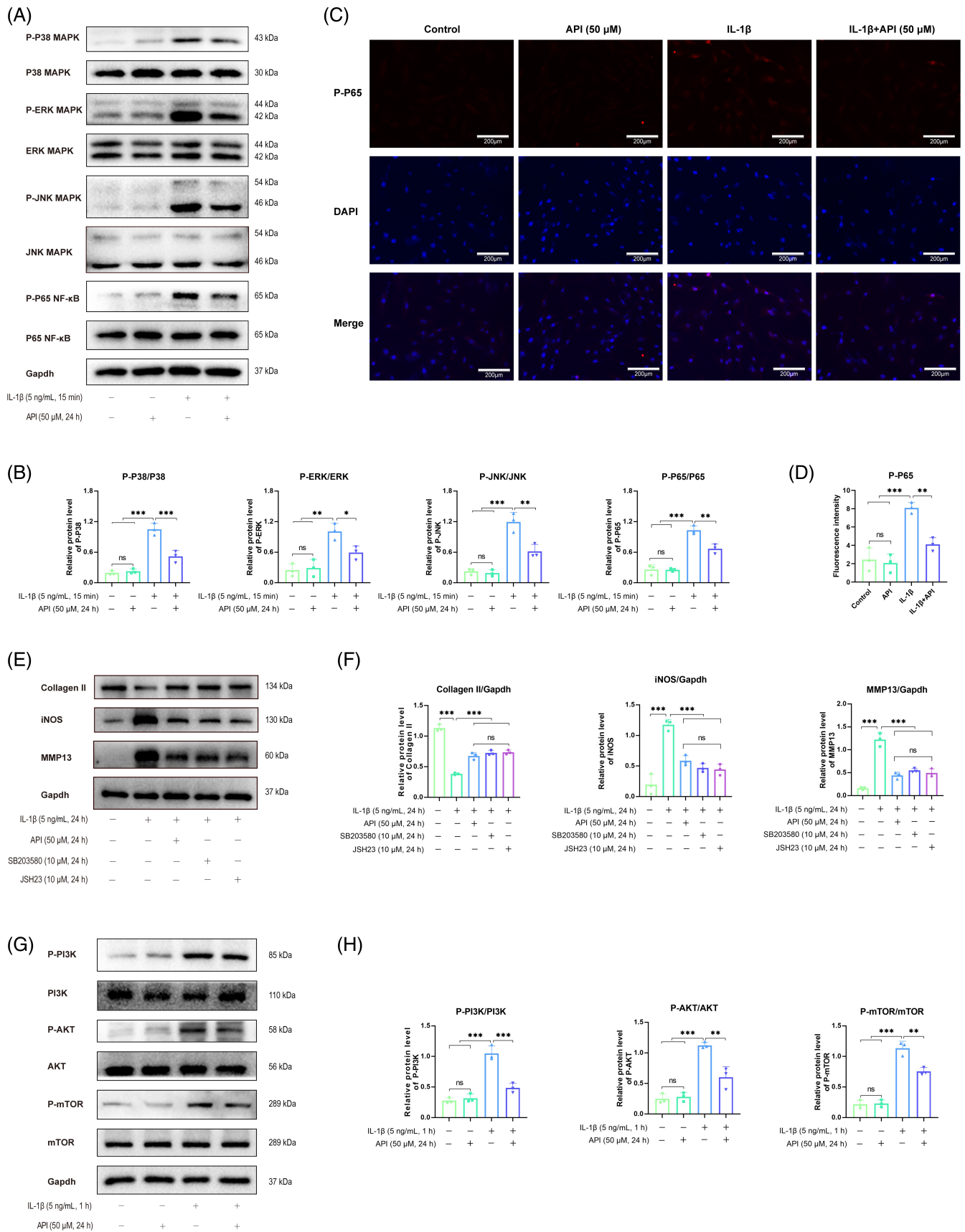


FIGURE 5 Legend on next page.

above, inflammation plays a vital role in the process of IVDD, including ECM degradation and innervation.^{52,53} Teixeira et al. fabricated nanoparticles with intrinsic anti-inflammatory characteristics to deliver an anti-inflammatory drug, diclofenac. After internalization of the drug-loaded nanoparticles, IL-1 β -treated IVD tissue showed a dramatic reduction in many inflammatory mediators (IL-6, IL-8, and PGE2), while remodeled ECM manifested by upregulation of ECM proteins (Collagen II and Aggrecan) and downregulation of matrix degrading enzymes (MMP1 and MMP3).⁵⁴ API shows excellent anti-inflammatory effects on various cell types, including skeletal muscle cells,⁵⁵ microglia,^{24,56} and adipocytes,⁵⁷ which makes it a promising treatment for inflammation-related diseases. Similarly, our results demonstrated that API significantly downregulated proinflammatory factors, which may further reduce catabolic activity while increasing anabolism in IL-1 β -stimulated NPCs. Multiple signaling pathways have been shown to be involved in IVDD. NF- κ B is one of the most well-known signaling pathways and is a central regulator of many inflammatory factors, such as TNF- α , IL-1 β , and IL-6.⁵⁸ MAPK signaling pathway plays a significant role in extracellular metabolism in IVD.⁵⁹ Disturbance of MAPK and NF- κ B pathways is believed to cause abnormal production of matrix-degrading enzymes such as MMPs and Aggrecans.⁴⁵ Our results demonstrate a prominent inhibition of the MAPK and NF- κ B signaling pathways after API administration, as supported by the reduced phosphorylation of P38, ERK, JNK, and P65 in IL-1 β -stimulated NPCs. These results indicate that API protects IVD from degeneration by regulating the abnormal phosphorylation of the MAPK and NF- κ B signaling pathway. Further studies are needed to elucidate the underlying mechanism.

After confirming the encouraging effects of API on inflammation, catabolism, anabolism, and associated signaling pathways, we further explored the biological processes mediated by API in NPCs. We identified the mediation of autophagy induced by API. The close association between autophagy and IVDD is well known. Tang et al. identified that nuclear factor (erythroid-derived-2)-like 2, a known regulator capable of protecting cells against oxidative stress, prevents IVD degeneration by inducing autophagy to combat oxidative stress.⁶⁰ Many biological molecules have been proven to prevent IVDD by enhancing autophagy.⁶¹⁻⁶³ Our results together with these studies confirm the mediating role of autophagy in IVDD. Consistent with a previous study,²⁷ our results revealed that API might enhance

autophagy by regulating the PI3K/AKT/mTOR signaling pathway. Elevated autophagy can be seen in NPCs in which the PI3K/AKT signaling pathway is inhibited.⁶⁴ mTOR exists in two different multi-subunit protein complexes: mTOR complex 1 (mTORC1) and mTOR complex 2 (mTORC2). Selective inhibition of mTORC1 prevents apoptosis, senescence, and catabolism in human NPCs.¹⁸ However, complete suppression of mTORC1 and mTORC2 would lead to apoptosis and senescence in human NPCs.¹⁹ In the current study, NPCs viability was not affected by API, which may be because API primarily inhibits mTORC1 rather than mTORC2. Future researches need to be performed to study the effect of API on mTORC1 and mTORC2 downstream genes. 3-MA is regarded as an effective autophagy inhibitor because it can inhibit class III PI3K. In addition, previous studies have proven that 3-MA has a dual role in autophagy.⁶⁵ 3-MA can inhibit autophagy under starving conditions, but promote autophagy under nutrient-rich conditions. In current experiment, NPCs were cultured in serum-free medium for 6 h, then replaced with complete medium and administered 3-MA. The results showed that 3-MA could inhibit the autophagy process of NPCs in the current experiment. The promotion of autophagy induced by API was not observed after 3-MA administration, which confirmed that API induced autophagy by inhibiting the PI3K/AKT/mTOR signaling pathway.

Although API has shown excellent anti-inflammatory and autophagy-promoting effects in vivo and in vitro study, further clinical applications still have some limitations to this study. First, one of the limitations is the absence of the utilization of accepted markers, Brachyury and CD24,⁶⁶ for the identification of rat NPCs in our study. Second, the assessment of oxygen concentration within the culture environment was not conducted. It is noteworthy that the nucleus pulposus cell resides in a hypoxic and avascular milieu, thus emphasizing the significance of monitoring the oxygen concentration in the culture environment. Third, we only use histomorphological and IHC analysis in in vivo study, whereas imageological examination remains to be performed. Forth, we only uncovered the impact of API on IVDD-related classical signaling pathways in this study. It is yet to be determined whether API exerts direct effects on these pathways or if its effects are indirect through other targets within these pathways. Fifth, we did not verify the therapeutic effect of API on human disk cells, which limited clinical relevance of this study. Despite these limitations, our research undeniably provides a potential theoretical basis for API applications to treat IVDD.

FIGURE 5 Apigetrin (API) inhibited the mitogen-activated protein kinase (MAPK), NF- κ B, and phosphatidylinositol 3-kinase (PI3K)/AKT/mammalian target of the rapamycin (mTOR) signaling pathways in interleukin-1 beta (IL-1 β)-stimulated nucleus pulposus cells (NPCs). (A, B) NF- κ B- and MAPK-related signaling molecules were analyzed by western blotting. (C) Immunofluorescence staining and (D) quantitative analysis of the nuclear translocation of P-P65 in NPCs. (E, F) The protein expression of inflammatory proteins (inducible nitric oxide synthase [iNOS]), anabolic proteins (Collagen II), and catabolic proteins (MMP13) in NPCs treated with IL-1 β (5 ng/mL) in the presence of API (10 μ M), or SB203580 (10 μ M), and or JSH23 (10 μ M). (G, H) The protein expression levels of PI3K/AKT/mTOR-related signaling molecules were analyzed by western blotting. Data are shown as the means \pm SD, $n = 3$. * $p < 0.05$; ** $p < 0.01$; *** $p < 0.001$. DAPI, 4,6-diamino-2-phenyl indole; ERK, extracellular signal-regulated kinase; JNK, c-Jun N-terminal kinase; LC3, light chain 3; ns, no significant difference; P-ERK, Phospho-ERK; P-JNK, Phospho-JNK; P-P65, Phospho-P65.

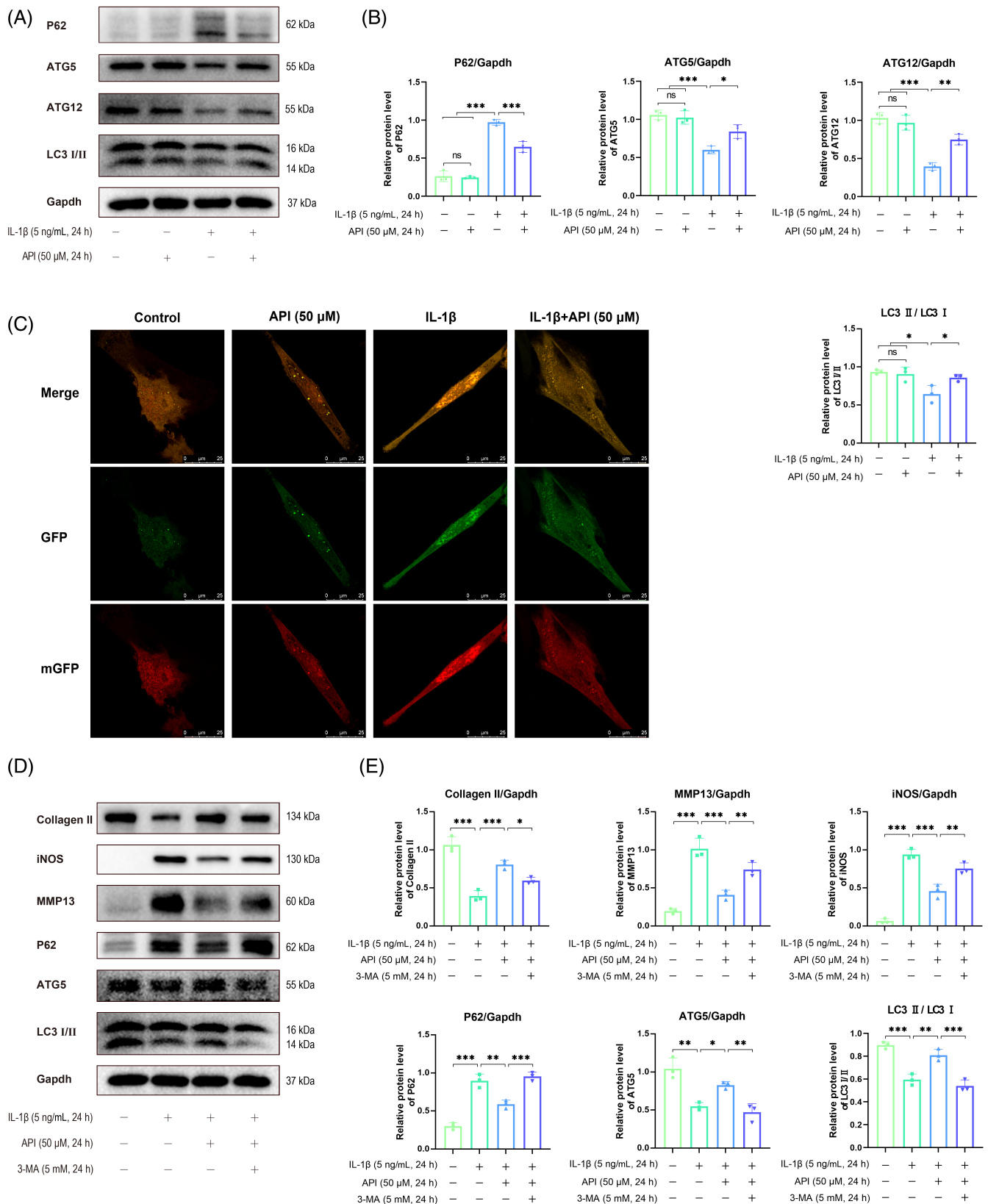


FIGURE 6 Apigenin (API) alleviated impaired autophagy in interleukin-1 beta (IL-1 β)-stimulated nucleus pulposus cells (NPCs). (A, B) Western blot analysis showed that the impaired autophagy induced by IL-1 β could be rescued by treatment with API (50 μ M). (C) NPCs were transfected with mRFP-GFP-LC3 adenovirus, and the strength of autophagic flux was captured with a confocal microscope. (D, E) The expression of autophagy-related proteins (P62, ATG5, and LC3II/I), inflammatory proteins (inducible nitric oxide synthase [iNOS]), anabolic proteins (Collagen II) and catabolic proteins (MMP13) in NPCs treated with or without 3-MA (5 mM) before treatment with API or IL-1 β . Data are shown as the means \pm SD, $n = 3$. * $p < 0.05$; ** $p < 0.01$; *** $p < 0.001$. ns, no significant difference.

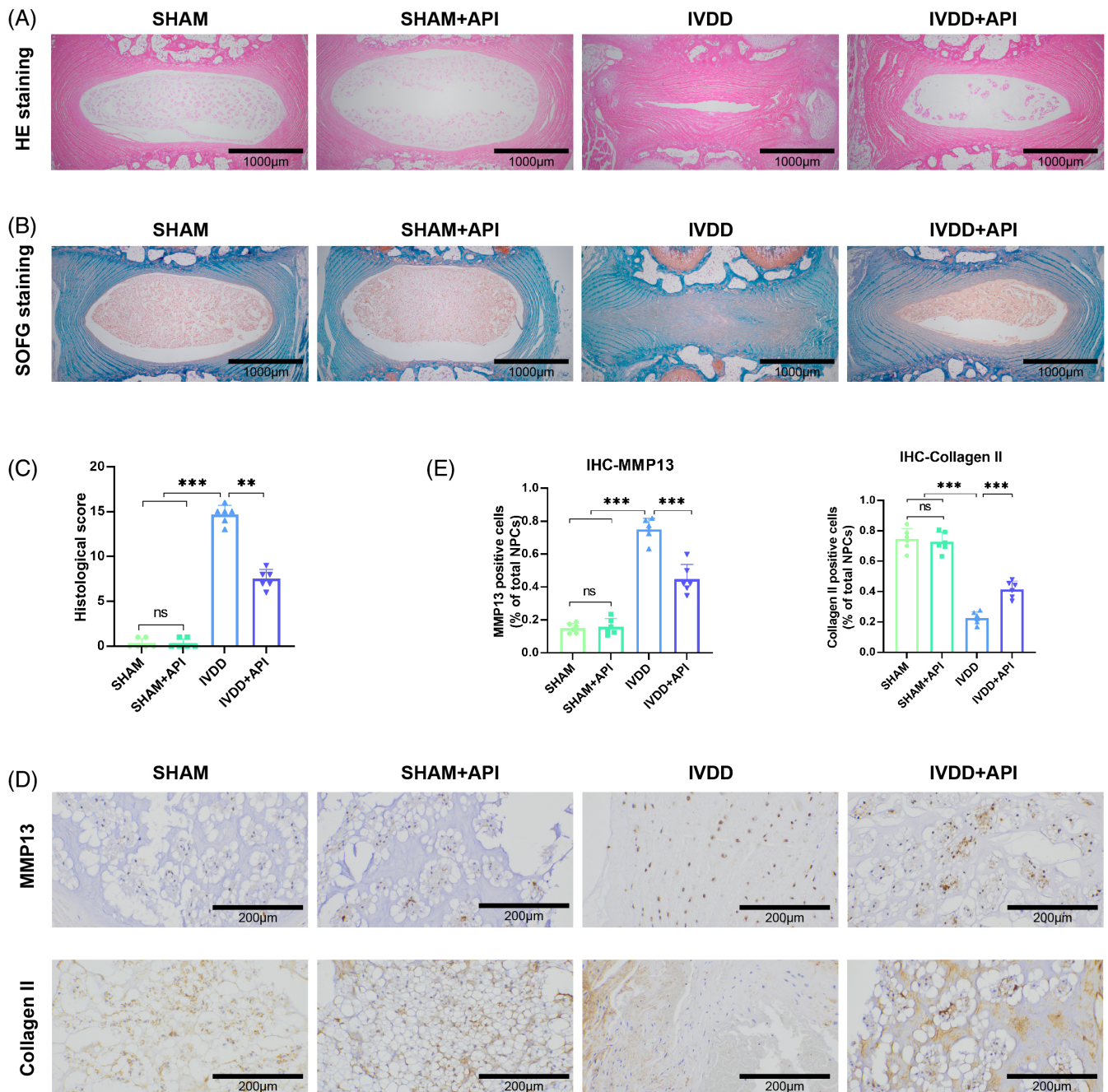


FIGURE 7 Apigetrin (API) ameliorated extracellular matrix (ECM) degeneration in a rat intervertebral disk degeneration (IVDD) model. (A) HE staining, (B) safranin O/fast green staining (SOFG), and (C) histological score evaluation. (D) Immunohistochemical (IHC) images of MMP13 and Collagen II and (E) the quantification of positive nucleus pulposus cells (NPCs). Data are shown as the means \pm SD, $n = 3$. ** $p < 0.01$; *** $p < 0.001$. ns, no significant difference.

5 | CONCLUSION

In short, as shown in Figure 8, API is capable of alleviating IVDD by inhibiting inflammation and balancing disturbed ECM homeostasis, which mainly relies on the improvement of autophagy in NPCs. Hence, we believe that API may be a promising candidate against LBP resulting from IVDD.

AUTHOR CONTRIBUTIONS

Conceptualization: Tao Xu, Hongqi Zhao, and Weihua Hu. *Data curation:* Tao Xu, Hongqi Zhao, Xuan Fang, Jian Li, Hua Wu, and Weihua Hu. *Formal analysis:* Jian Li and Xuan Fang. *Funding acquisition:* Weihua Hu; *Methodology,* Tao Xu, Hongqi Zhao, and Jian Li. *Project administration:* Tao Xu, Hongqi Zhao, Weihua Hu; *Software,* Xuan Fang, and Jian Li. *Supervision:* Hua Wu and Weihua Hu. *Validation:*

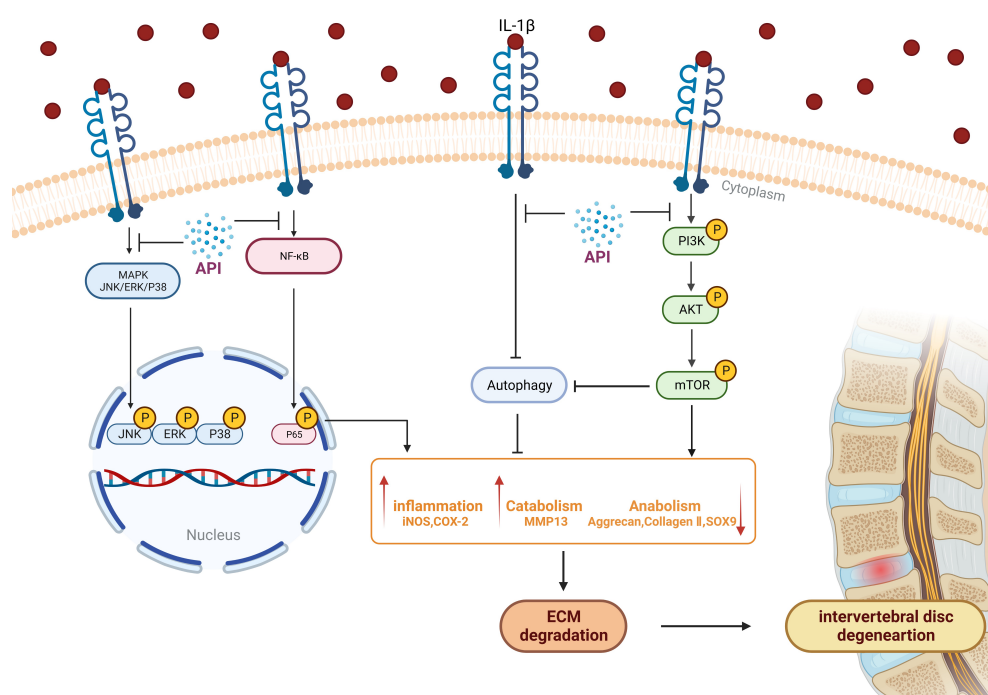


FIGURE 8 Schematic illustration of the potential protective effects of Apigetrin (API) on the progression of intervertebral disk degeneration (Source: figure was created in BioRender.com). ECM, extracellular matrix; ERK, extracellular signal-regulated kinase; IL-1 β , interleukin-1 beta; iNOS, inducible nitric oxide synthase; JNK, c-Jun N-terminal kinase; mTOR, mammalian target of the rapamycin; P13K, phosphatidylinositol 3-kinase.

Hua Wu, Jian Li; Visualization, Xuan Fang, Jian Li. Writing—original draft: Tao Xu and Hongqi Zhao. Writing—review & editing: Tao Xu, Hongqi Zhao, and Weihua Hu.

ACKNOWLEDGMENTS

The authors show sincere gratitude for the support of [BioRender.com](https://www.biorender.com).

FUNDING INFORMATION

This research was supported by Hubei Provincial Natural Science Foundation of China (2023AFB646) and Knowledge Innovation Program of Wuhan-Basic Research (2023020201010155).

CONFLICT OF INTEREST STATEMENT

All authors declare that they have no conflict of interest.

DATA AVAILABILITY STATEMENT

The data supporting the findings are presented in the article, further inquiries can be directed to the corresponding author.

ORCID

Weihua Hu  <https://orcid.org/0000-0003-4813-0069>

REFERENCES

- Kent P, Haines T, O'Sullivan P, et al. Cognitive functional therapy with or without movement sensor biofeedback versus usual care for chronic, disabling low back pain (RESTORE): a randomised, controlled, three-arm, parallel group, phase 3, clinical trial. *Lancet*. 2023;401(10391):1866-1877.
- Hartvigsen J, Hancock MJ, Kongsted A, et al. What low back pain is and why we need to pay attention. *Lancet*. 2018;391(10137):2356-2367.
- Dieleman JL, Cao J, Chapin A, et al. US health care spending by payer and health condition, 1996-2016. *JAMA*. 2020;323(9):863-884.
- Zhang S, Hu B, Liu W, et al. The role of structure and function changes of sensory nervous system in intervertebral disc-related low back pain. *Osteoarthritis Cartilage*. 2021;29(1):17-27.
- Luoma K, Riihimäki H, Luukkonen R, Raininko R, Viikari-Juntura E, Lamminen A. Low back pain in relation to lumbar disc degeneration. *Spine*. 2000;25(4):487-492.
- Clouet J, Fusellier M, Camus A, Le Visage C, Guicheux J. Intervertebral disc regeneration: from cell therapy to the development of novel bioinspired endogenous repair strategies. *Adv Drug Deliv Rev*. 2019;146:306-324.
- Chen D, Xia D, Pan Z, et al. Metformin protects against apoptosis and senescence in nucleus pulposus cells and ameliorates disc degeneration in vivo. *Cell Death Dis*. 2016;7(10):e2441.
- Clouet J, Vinatier C, Merceron C, et al. The intervertebral disc: from pathophysiology to tissue engineering. *Joint Bone Spine*. 2009;76(6):614-618.
- Li G, Zhang W, Liang H, Yang C. Epigenetic regulation in intervertebral disc degeneration. *Trends Mol Med*. 2022;28(10):803-805.
- Fontana G, See E, Pandit A. Current trends in biologics delivery to restore intervertebral disc anabolism. *Adv Drug Deliv Rev*. 2015;84:146-158.
- Ge Q, Ying J, Shi Z, Mao Q, et al. Chlorogenic acid retards cartilaginous endplate degeneration and ameliorates intervertebral disc degeneration via suppressing NF- κ B signaling. *Life Sci*. 2021;274:119324.
- Vo NV, Hartman RA, Yurube T, Jacobs LJ, Sowa GA, Kang JD. Expression and regulation of metalloproteinases and their inhibitors in intervertebral disc aging and degeneration. *Spine J*. 2013;13(3):331-341.
- Rubinsztein DC, Mariño G, Kroemer G. Autophagy and aging. *Cell*. 2011;146(5):682-695.
- Madeo F, Tavernarakis N, Kroemer G. Can autophagy promote longevity. *Nat Cell Biol*. 2010;12(9):842-846.
- Wang J, Zhang Y, Cao J, et al. The role of autophagy in bone metabolism and clinical significance. *Autophagy*. 2023;19(9):2409-2427.
- Wang Y, Shen J, Chen Y, et al. PINK1 protects against oxidative stress induced senescence of human nucleus pulposus cells via regulating mitophagy. *Biochem Biophys Res Commun*. 2018;504(2):406-414.

17. Hu S, Chen L, Al Mamun A, Ni L, et al. The therapeutic effect of TBK1 in intervertebral disc degeneration via coordinating selective autophagy and autophagic functions. *J Adv Res.* 2021;30:1-13.
18. Ito M, Yurube T, Kakutani K, et al. Selective interference of mTORC1/RAPTOR protects against human disc cellular apoptosis, senescence, and extracellular matrix catabolism with AKT and autophagy induction. *Osteoarthr Cartil.* 2017;25(12):2134-2146.
19. Kakiuchi Y, Yurube T, Kakutani K, et al. Pharmacological inhibition of mTORC1 but not mTORC2 protects against human disc cellular apoptosis, senescence, and extracellular matrix catabolism through AKT and autophagy induction. *Osteoarthr Cartil.* 2019;27(6):965-976.
20. Yurube T, Ito M, Kakiuchi Y, Kuroda R, Kakutani K. Autophagy and mTOR signaling during intervertebral disc aging and degeneration. *JOR Spine.* 2020;3(1):e1082.
21. Yu H, Teng Y, Ge J, et al. Isoginkgetin-loaded reactive oxygen species scavenging nanoparticles ameliorate intervertebral disc degeneration via enhancing autophagy in nucleus pulposus cells. *J Nanobiotechnol.* 2023;21(1):99.
22. Xie L, Huang W, Fang Z, et al. CircERCC2 ameliorated intervertebral disc degeneration by regulating mitophagy and apoptosis through miR-182-5p/SIRT1 axis. *Cell Death Dis.* 2019;10(10):751.
23. Xu P, Marsafari M, Zha J, Koffas M. Microbial coculture for flavonoid synthesis. *Trends Biotechnol.* 2020;38(7):686-688.
24. Lim HS, Kim OS, Kim BY, Jeong SJ. Apigenin from *Scutellaria baicalensis* Georgi inhibits neuroinflammation in BV-2 microglia and exerts neuroprotective effect in HT22 hippocampal cells. *J Med Food.* 2016;19(11):1032-1040.
25. Zhang R, Shi J, Wang T, et al. Apigenin ameliorates streptozotocin-induced pancreatic β -cell damages via attenuating endoplasmic reticulum stress. *In Vitro Cell Dev Biol Anim.* 2020;56(8):622-634.
26. Guo H, Li M, Xu LJ. Apigenin treatment attenuates LPS-induced acute otitis media through suppressing inflammation and oxidative stress. *Biomed Pharmacother.* 2019;109:1978-1987.
27. Kim SM, Vettrivel P, Ha SE, Kim HH, Kim JA, Kim GS. Apigenin induces extrinsic apoptosis, autophagy and G2/M phase cell cycle arrest through PI3K/AKT/mTOR pathway in AGS human gastric cancer cell. *J Nutr Biochem.* 2020;83:108427.
28. Lu R, Xu H, Deng X, Wang Y, et al. Physalin a alleviates intervertebral disc degeneration via anti-inflammatory and anti-fibrotic effects. *J Orthop Translat.* 2023;39:74-87.
29. Yurube T, Takada T, Hirata H, et al. Modified house-keeping gene expression in a rat tail compression loading-induced disc degeneration model. *J Orthop Res.* 2011;29(8):1284-1290.
30. Han B, Zhu K, Li FC, et al. A simple disc degeneration model induced by percutaneous needle puncture in the rat tail. *Spine.* 2008;33(18):1925-1934.
31. Qian J, Ge J, Yan Q, Wu C, Yang H, Zou J. Selection of the optimal puncture needle for induction of a rat intervertebral disc degeneration model. *Pain Physician.* 2019;22(4):353-360.
32. Mao HJ, Chen QX, Han B, et al. The effect of injection volume on disc degeneration in a rat tail model. *Spine.* 2011;36(16):E1062-E1069.
33. Lai A, Gansau J, Gullbrand SE, et al. Development of a standardized histopathology scoring system for intervertebral disc degeneration in rat models: an initiative of the ORS spine section. *JOR Spine.* 2021;4(2):e1150.
34. Shnyder NA, Ashkhotov AV, Trefilova VV, et al. Cytokine imbalance as a biomarker of intervertebral disk degeneration. *Int J Mol Sci.* 2023;24(3):2360.
35. Shnyder NA, Ashkhotov AV, Trefilova VV, et al. Molecular basic of pharmacotherapy of cytokine imbalance as a component of intervertebral disc degeneration treatment. *Int J Mol Sci.* 2023;24(9):7692.
36. Zou X, Zhang X, Han S, Wei L, et al. Pathogenesis and therapeutic implications of matrix metalloproteinases in intervertebral disc degeneration: a comprehensive review. *Biochimie.* 2023;214(pt B):27-48.
37. Kibble MJ, Domingos M, Hoyland JA, Richardson SM. Importance of matrix cues on intervertebral disc development, degeneration, and regeneration. *Int J Mol Sci.* 2022;23(13):6915.
38. Zhang GZ, Liu MQ, Chen HW, et al. NF- κ B signalling pathways in nucleus pulposus cell function and intervertebral disc degeneration. *Cell Prolif.* 2021;54(7):e13057.
39. Zhang HJ, Liao HY, Bai DY, Wang ZQ, Xie XW. MAPK/ERK signaling pathway: a potential target for the treatment of intervertebral disc degeneration. *Biomed Pharmacother.* 2021;143:112170.
40. Gong Y, Qiu J, Jiang T, et al. Maltol ameliorates intervertebral disc degeneration through inhibiting PI3K/AKT/NF- κ B pathway and regulating NLRP3 inflammasome-mediated pyroptosis. *Inflammopharmacology.* 2023;31(1):369-384.
41. Kritschil R, Scott M, Sowa G, Vo N. Role of autophagy in intervertebral disc degeneration. *J Cell Physiol.* 2022;237(2):1266-1284.
42. Livshits G, Popham M, Malkin I, et al. Lumbar disc degeneration and genetic factors are the main risk factors for low back pain in women: the UK twin spine study. *Ann Rheum Dis.* 2011;70(10):1740-1745.
43. Millecamps M, Tajarier M, Naso L, Sage HE, Stone LS. Lumbar intervertebral disc degeneration associated with axial and radiating low back pain in ageing SPARC-null mice. *Pain.* 2012;153(6):1167-1179.
44. Park EH, Moon SW, Suh HR, et al. Disc degeneration induces a mechano-sensitization of disc afferent nerve fibers that associates with low back pain. *Osteoarthr Cartil.* 2019;27(11):1608-1617.
45. Sakai D, Grad S. Advancing the cellular and molecular therapy for intervertebral disc disease. *Adv Drug Deliv Rev.* 2015;84:159-171.
46. Novais EJ, Tran VA, Johnston SN, Darris KR, et al. Long-term treatment with senolytic drugs dasatinib and quercetin ameliorates age-dependent intervertebral disc degeneration in mice. *Nat Commun.* 2021;12(1):5213.
47. Shao Z, Wang B, Shi Y, et al. Senolytic agent quercetin ameliorates intervertebral disc degeneration via the Nrf2/NF- κ B axis. *Osteoarthr Cartil.* 2021;29(3):413-422.
48. Wang D, He X, Wang D, et al. Quercetin suppresses apoptosis and attenuates intervertebral disc degeneration via the SIRT1-autophagy pathway. *Front Cell Dev Biol.* 2020;8:613006.
49. Xie C, Ma H, Shi Y, et al. Cardamonin protects nucleus pulposus cells against IL-1 β -induced inflammation and catabolism via Nrf2/NF- κ B axis. *Food Funct.* 2021;12(6):2703-2714.
50. Fang W, Zhou X, Wang J, Xu L, et al. Wogonin mitigates intervertebral disc degeneration through the Nrf2/ARE and MAPK signaling pathways. *Int Immunopharmacol.* 2018;65:539-549.
51. Fuchs J, Milbradt R. Skin anti-inflammatory activity of apigenin-7-glucoside in rats. *Arzneimittelforschung.* 1993;43(3):370-372.
52. Kang L, Zhang H, Jia C, Zhang R, Shen C. Epigenetic modifications of inflammation in intervertebral disc degeneration. *Ageing Res Rev.* 2023;87:101902.
53. Lee JM, Song JY, Baek M, et al. Interleukin-1 β induces angiogenesis and innervation in human intervertebral disc degeneration. *J Orthop Res.* 2011;29(2):265-269.
54. Teixeira GQ, Leite Pereira C, Castro F, et al. Anti-inflammatory chitosan/poly- γ -glutamic acid nanoparticles control inflammation while remodeling extracellular matrix in degenerated intervertebral disc. *Acta Biomater.* 2016;42:168-179.
55. Ha SE, Bhagwan Bhosale P, Kim HH, et al. Apigenin abrogates lipopolysaccharide-induced inflammation in L6 skeletal muscle cells through NF- κ B/MAPK signaling pathways. *Curr Issues Mol Biol.* 2022;44(6):2635-2645.
56. Bian M, Zhang Y, Du X, Xu J, et al. Apigenin-7-digluconide protects retinas against bright light-induced photoreceptor degeneration through the inhibition of retinal oxidative stress and inflammation. *Brain Res.* 2017;1663:141-150.
57. Hadrich F, Sayadi S. Apigenin inhibits adipogenesis in 3T3-L1 cells by downregulating PPAR γ and CEBP- α . *Lipids Health Dis.* 2018;17(1):95.

58. Capece D, Verzella D, Flati I, Arboretto P, Cornice J, Franzoso G. NF- κ B: blending metabolism, immunity, and inflammation. *Trends Immunol.* 2022;43(9):757-775.
59. Hiyama A, Sakai D, Mochida J. Cell signaling pathways related to pain receptors in the degenerated disk. *Global Spine J.* 2013;3(3):165-174.
60. Tang Z, Hu B, Zang F, Wang J, Zhang X, Chen H. Nrf2 drives oxidative stress-induced autophagy in nucleus pulposus cells via a Keap1/Nrf2/p62 feedback loop to protect intervertebral disc from degeneration. *Cell Death Dis.* 2019;10(7):510.
61. Chen F, Liu H, Wang X, et al. Melatonin activates autophagy via the NF- κ B signaling pathway to prevent extracellular matrix degeneration in intervertebral disc. *Osteoarthr Cartil.* 2020;28(8):1121-1132.
62. Zuo R, Wang Y, Li J, Wu J, et al. Rapamycin induced autophagy inhibits inflammation-mediated endplate degeneration by enhancing Nrf2/Keap1 signaling of cartilage endplate stem cells. *Stem Cells.* 2019;37(6):828-840.
63. Chen Y, Zheng Z, Wang J, et al. Berberine suppresses apoptosis and extracellular matrix (ECM) degradation in nucleus pulposus cells and ameliorates disc degeneration in a rodent model. *Int Aust J Biol Sci.* 2018;14(6):682-692.
64. Guo F, Zou Y, Zheng Y. Moracin M inhibits lipopolysaccharide-induced inflammatory responses in nucleus pulposus cells via regulating PI3K/AKT/mTOR phosphorylation. *Int Immunopharmacol.* 2018; 58:80-86.
65. Wu YT, Tan HL, Shui G, et al. Dual role of 3-methyladenine in modulation of autophagy via different temporal patterns of inhibition on class I and III phosphoinositide 3-kinase. *J Biol Chem.* 2010;285(14): 10850-10861.
66. Risbud MV, Schoepflin ZR, Mwale F, et al. Defining the phenotype of young healthy nucleus pulposus cells: recommendations of the spine research interest group at the 2014 annual ORS meeting. *J Orthop Res.* 2015;33(3):283-293.

How to cite this article: Xu T, Zhao H, Li J, Fang X, Wu H, Hu W. Apigetrin alleviates intervertebral disk degeneration by regulating nucleus pulposus cell autophagy. *JOR Spine.* 2024; 7(2):e1325. doi:[10.1002/jsp2.1325](https://doi.org/10.1002/jsp2.1325)